Electronic Supplementary Information

Slow magnetic relaxation of mononuclear complexes based on uncommon Kramers lanthanide ions Ce^{III}, Sm^{III} and Yb^{III}

Ji-Dong Leng,[a] Qiu-Yan Hua,[a] Wen-Ting Liu,[b] Ze-Xian Tao,[a] Nai-Wen Tan,[a] Yu-Fei Wang,[a] Wei-Quan Lin*[a]

Table S1. Crystal data and structure refinement for **1**-**3**.

	1	**2**	**3**
Empirical formula	$C_{68}H_{66}Cl_3O_7P_4Ce$	$C_{68}H_{66}Cl_3O_7P_4Sm$	$C_{64}H_{60}Cl_3O_7P_4Yb$
Formula weight	1365.64	1375.92	1344.47
Temperature/K	100.00(10)	105(8)	99.99(10)
Crystal system	triclinic	triclinic	triclinic
Space group	*P*-1	*P*-1	*P*-1
a [Å]	11.32160(10)	11.3010(2)	13.50187(5)
b [Å]	12.4712(2)	12.4404(2)	14.30058(5)
c [Å]	22.4085(2)	22.2903(2)	15.59805(6)
α [°]	98.4460(10)	98.8240(10)	91.4607(3)
β [°]	94.3080(10)	93.9410(10)	101.8219(3)
γ [°]	114.7660(10)	114.9520(10)	95.1610(3)
Volume [Å^3]	2808.70(6)	2776.32(7)	2932.928(19)
Z	2	2	2
Density (calcd) [g cm^{-3}]	1.423	1.452	1.522
μ [mm^{-1}]	9.014	10.725	5.671
F(000)	1218.0	1226.0	1362.0
2*Θ* range for data collection [°]	8.188 to 154.712	8.118 to 153.64	5.794 to 154.162
Reflections collected	36815	36235	84890
Independent reflections	11409 (R_{int} = 0.0447, R_{sigma} = 0.0447)	11244 (R_{int} = 0.0393, R_{sigma} = 0.0381)	11944 (R_{int} = 0.0332, R_{sigma} = 0.0174)
Goodness-of-fit on F^2	1.070	1.058	1.067
Final *R* indexes [$I \geq 2\sigma(I)$]	R_1 = 0.0380, wR_2 = 0.0961	R_1 = 0.0303, wR_2 = 0.0772	R_1 = 0.0363, wR_2 = 0.0984
Final *R* indexes [all data]	R_1 = 0.0401, wR_2 = 0.0973	R_1 = 0.0312, wR_2 = 0.0777	R_1 = 0.0367, wR_2 = 0.0987
Largest diff. peak and hole [e Å^{-3}]	1.43 and -0.85	0.63 and -0.71	2.25 and -2.27

Table S2. Selected bond lengths (Å) and angles (°) for **1**-**3**.

1					
Ce(1)-Cl(1)	2.8053(10)	Ce(1)-Cl(2)	2.7805(9)	Ce(1)-Cl(3)	2.7954(11)
Ce(1)-O(1)	2.389(2)	Ce(1)-O(2)	2.477(2)	Ce(1)-O(3)	2.435(2)
Ce(1)-O(4)	2.427(2)				
Cl(1)-Ce(1)-O(2)	80.73(6)	Cl(1)-Ce(1)-O(3)	118.54(6)	Cl(1)-Ce(1)-O(4)	78.55(6)
Cl(2)-Ce(1)-Cl(3)	110.72(3)	Cl(2)-Ce(1)-O(1)	77.68(6)	Cl(2)-Ce(1)-O(2)	143.29(6)
Cl(2)-Ce(1)-O(3)	79.92(6)	Cl(2)-Ce(1)-O(4)	128.32(6)	Cl(3)-Ce(1)-O(1)	82.04(6)

Cl(3)-Ce(1)-O(2)	80.43(6)	Cl(3)-Ce(1)-O(3)	78.50(6)	Cl(3)-Ce(1)-O(4)	101.80(6)
O(1)-Ce(1)-O(2)	69.19(7)	O(1)-Ce(1)-O(3)	142.70(8)	O(1)-Ce(1)-O(4)	147.59(8)
O(2)-Ce(1)-O(3)	136.65(8)	O(2)-Ce(1)-O(4)	79.65(8)	O(3)-Ce(1)-O(4)	68.32(8)
2					
Sm1-Cl1	2.7443(8)	Sm1-Cl2	2.7217(8)	Sm1-Cl3	2.7375(9)
Sm1-O1	2.363(2)	Sm1-O2	2.372(2)	Sm1-O3	2.331(2)
Sm1-O4	2.410(2)				
Cl1-Sm1-O2	78.51(5)	Cl1-Sm1-O3	88.42(5)	Cl1-Sm1-O4	81.71(5)
Cl2-Sm1-Cl3	110.26(2)	Cl2-Sm1-O1	78.56(5)	Cl2-Sm1-O2	128.81(6)
Cl2-Sm1-O3	77.48(5)	Cl2-Sm1-O4	144.45(5)	Cl3-Sm1-O1	78.47(6)
Cl3-Sm1-O2	101.39(5)	Cl3-Sm1-O3	82.21(5)	Cl3-Sm1-O4	80.53(5)
O1-Sm1-O2	69.45(6)	O1-Sm1-O3	141.57(7)	O1-Sm1-O4	136.84(7)
O2-Sm1-O3	147.66(7)	O2-Sm1-O4	78.43(7)	O3-Sm1-O4	70.42(7)
3					
Yb1-Cl1	2.5519(8)	Yb1-Cl2	2.5541(8)	Yb1-O1	2.223(2)
Yb1-O2	2.220(2)	Yb1-O3	2.200(2)	Yb1-O4	2.206(2)
Cl1-Yb1-Cl2	97.35(3)	Cl1-Yb1-O1	91.45(6)	Cl1-Yb1-O2	94.04(6)
Cl1-Yb1-O3	166.98(6)	Cl1-Yb1-O4	93.58(6)	Cl2-Yb1-O1	169.73(6)
Cl2-Yb1-O2	95.86(6)	Cl2-Yb1-O3	91.15(6)	Cl2-Yb1-O4	90.22(6)
O1-Yb1-O2	78.18(8)	O1-Yb1-O3	81.13(8)	O1-Yb1-O4	94.51(8)
O2-Yb1-O3	94.89(8)	O2-Yb1-O4	169.56(8)	O3-Yb1-O4	76.47(8)

Table S3. Continuous Shape Measures Calculations for **1** and **2**.

Ideal structures			CShM values for **1**	CShM values for **2**
HP-7	D_{7h}	Square	35.12419	35.29980
HPY-7	C_{6v}	Tetrahedron	19.68524	20.17462
PBPY-7	D_{5h}	D5h	4.53044	4.33962
COC-7	C_{3v}	Capped octahedron	1.93484	2.00211
CTPR-7	C_{2v}	Capped trigonal prism	1.91561	1.90172
JPBPY-7	D_{5h}	Johnson pentagonal bipyramid J13	9.99254	9.88358
JETPY-7	C_{3v}	Johnson elongated triangular pyramid J7	20.98252	21.35009

Table S4. Continuous Shape Measures Calculations for **3**.

Ideal structures			CShM values for **3**
HP-6	D_{6h}	Hexagon	30.45376
PPY-6	C_{5v}	Pentagonal pyramid	24.91418
OC-6	O_h	Octahedron	1.59423
TPR-6	D_{3h}	Trigonal prism	14.40012
JPPY-6	C_{5v}	Johnson pentagonal pyramid J2	29.95800

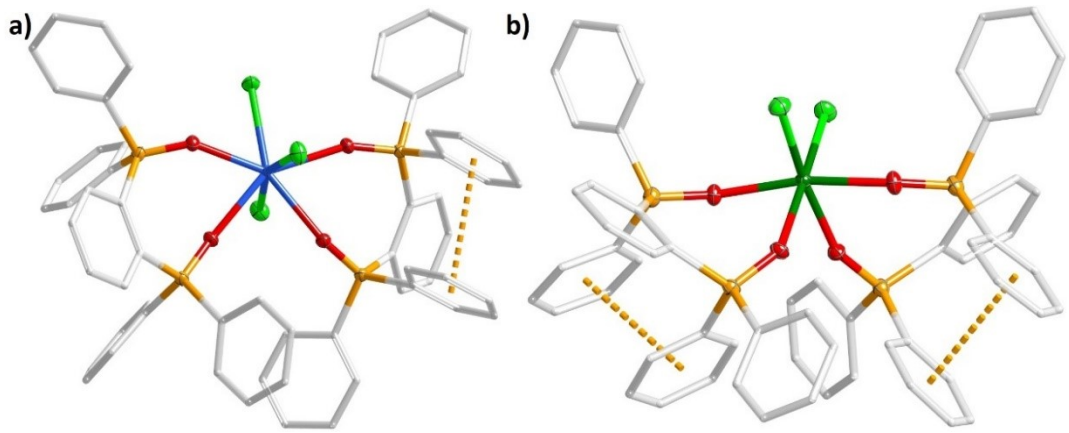

Figure S1. The molecule structure of complexes **2** (a) and **3** (b) showing the intramolecular π-π interaction.

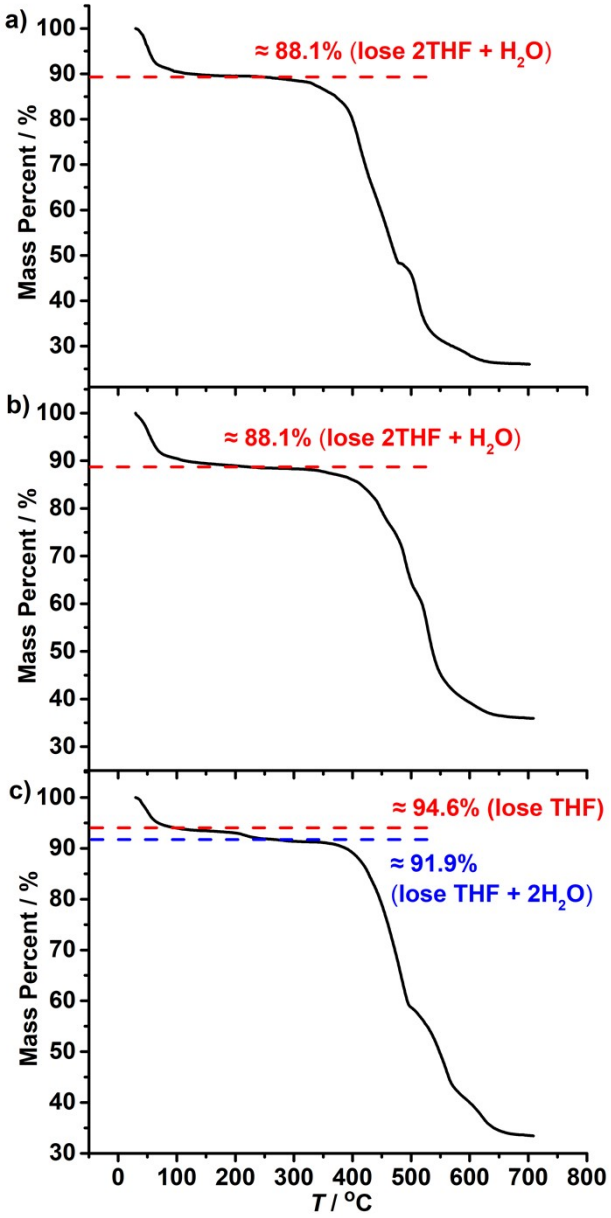

Figure S2. TG analyses for **1** (a), **2** (b) and **3** (c).

Table S5. Esd calculations on the two phenyl (Ph) rings with *π*-*π* interactions for **1**-**3**.

	1	**2**	Interaction 1 of **3**	Interaction 2 of **3**
Ph1	C37-C42	C37-C42	C7-C12	C37-C42
Ph2	C49-C54	C55-C60	C19-C24	C49-C54
Centroid-centroid distance	3.674	3.650	3.554	3.752
Shift distance	1.470	1.402	1.251	1.065
Dihedral angle	6.72	5.86	4.88	5.42
Ph1 to Ph2 centroid distance	3.515	3.370	3.406	3.597
Ph2 to Ph1 centroid distance	3.366	3.495	3.327	3.633

Both 'pipi' command in OLEX2[1] and PLATON[2] checking suggest intramolecular face-to-face *π*-*π* interactions for 1-3 as were show in Table S5. Moreover, detail geometric parameters of the interacting phenyl rings were calculated based on the single-crystal structures. The obtained results are in reasonable range and confirmed the intramolecular face-to-face *π*-*π* interactions.[3, 4]

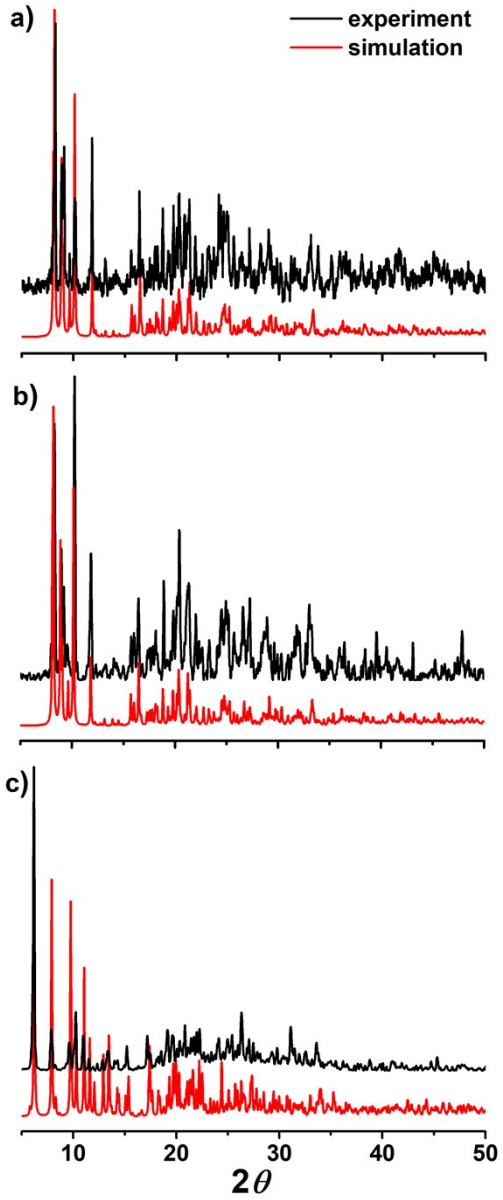

Figure S3. Experimental (black) and simulated (red) powder X-ray diffraction patterns of complexes **1** (a), **2** (b) and **3** (c).

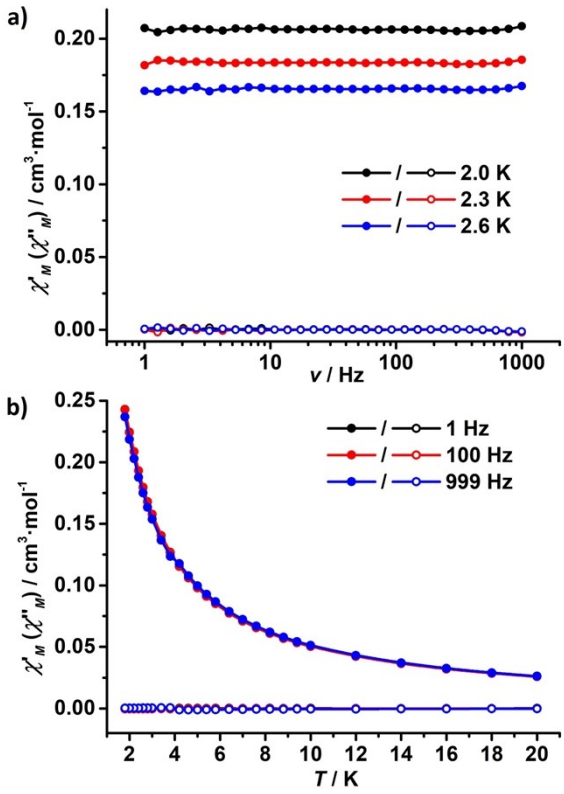

Figure S4. Frequency (a) and temperature (b) dependent in-phase (χ'_M, solid circles) and out-of-phase (χ''_M, open circles) ac magnetic susceptibility plots for complex **1** under a zero external magnetic field. The solid lines are only a guide for the eyes.

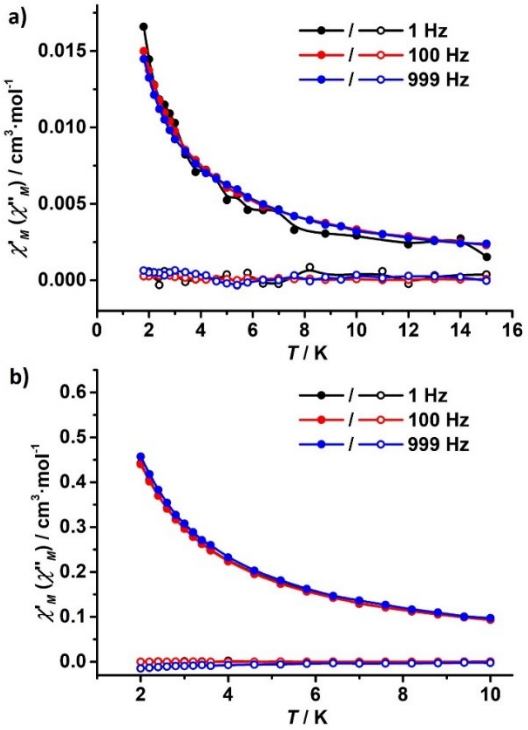

Figure S5. Temperature dependent in-phase (χ'_M, solid circles) and out-of-phase (χ''_M, open circles) ac magnetic susceptibility plots for complex **2** (a) and **3** (b) under a zero external magnetic field. The solid lines are only a guide for the eyes.

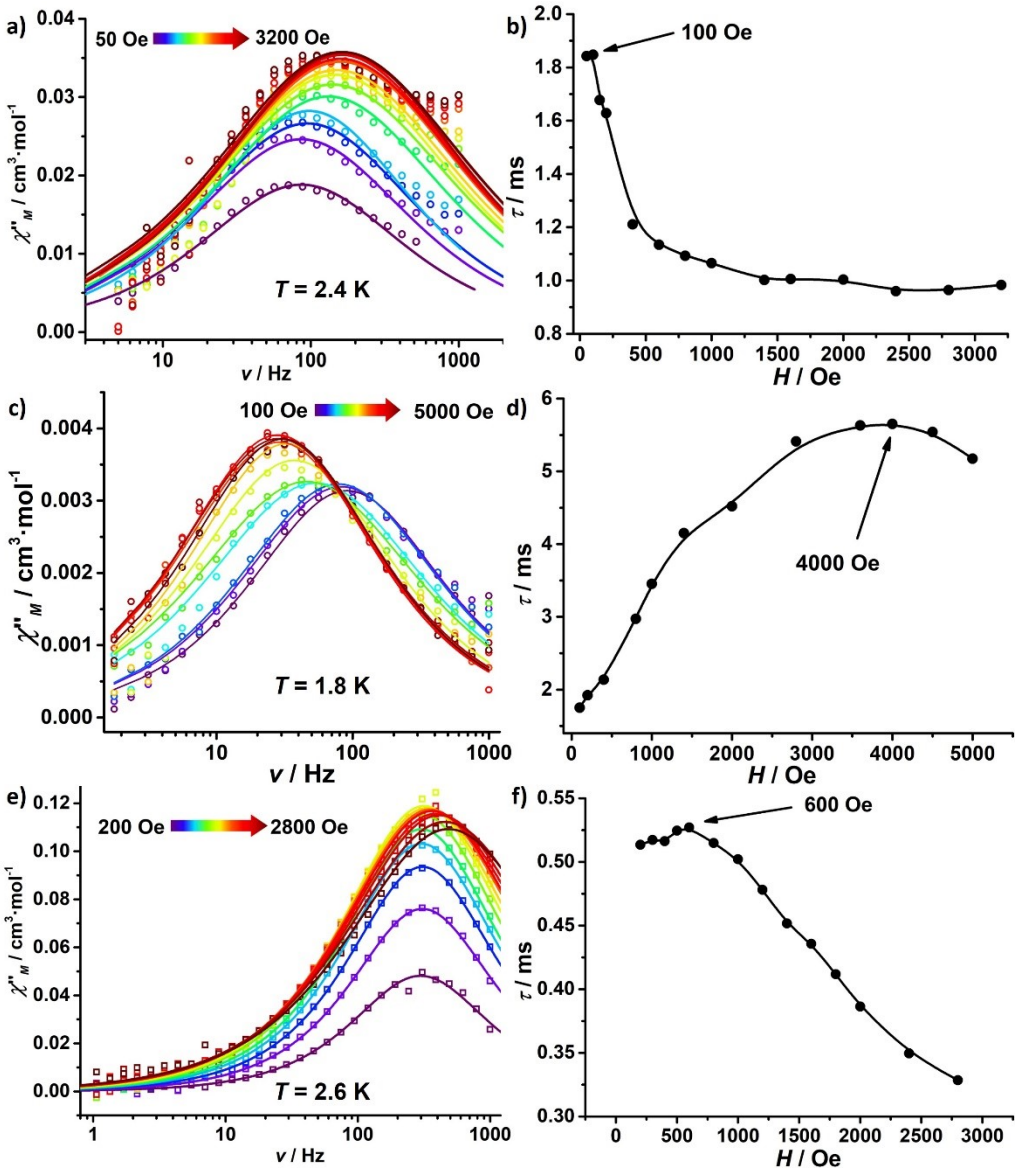

Figure S6. Frequency dependent out-of-phase (χ''_M) ac magnetic susceptibility (left) and field dependent relaxation times (right) for complex **1** (top), **2** (middle) and **3** (bottom) under various dc fields, at indicated temperatures. The chromatic solid lines (left) represent the fitting results using Debye model, and the black lines (right) are only a guide for the eyes.

Table S6. CASSCF computed spin-free and spin-orbit state energies for **1** - **3**.

Spin-free Energies (cm^{-1})			Spin-Orbit states (cm^{-1})		
1	**2**	**3**	**1**	**2**	**3**
0	0	0	0	0	0
60.237	23.353	162.789	0	0	0
261.643	45.025	238.493	290.785	63.509	136.618
354.879	75.527	353.488	290.785	63.509	136.618
449.163	109.875	503.746	501.144	198.923	312.267
683.612	121.263	601.420	501.144	198.923	312.267
886.066	276.913	671.865	2360.776	886.786	495.315
……	303.442	……	2360.776	886.786	495.315

319.428	2551.039	951.326	10387.371
426.378	2551.039	951.326	10387.371
443.197	2727.929	995.996	10504.428
6776.927	2727.929	995.996	10504.428
……	3012.712	1063.127	10786.612
	3012.712	1063.127	10786.612
		2008.452	
		2008.452	
		……	

Table S7. Wavefunctions composition for each | m_J 〉 state of the ground-state multiples for **1** - **3**.

	KDs	Wave functions
1	1	53.2%|±5/2〉+ 26.5%|±3/2〉+ 20.2%|±1/2〉
	2	20.4%|±5/2〉+ 25.4%|±3/2〉+ 54.1%|±1/2〉
	3	26.4%|±5/2〉+ 48.1%|±3/2〉+ 25.5%|±1/2〉
2	1	65.0%|±5/2〉+ 6.7%|±3/2〉+ 28.4%|±1/2〉
	2	16.3%|±5/2〉+ 29.9%|±3/2〉+ 53.8%|±1/2〉
	3	18.8%|±5/2〉+ 63.5%|±3/2〉+ 17.8%|±1/2〉
3	1	40.2%|±7/2〉+ 33.9%|±5/2〉+ 9.7|±3/2〉+ 16.1%|±1/2〉
	2	39.4%|±7/2〉+ 35.3%|±5/2〉+ 22.5|±3/2〉+ 2.9%|±1/2〉
	3	4.6%|±7/2〉+ 19.9%|±5/2〉+ 42.7|±3/2〉+ 32.8%|±1/2〉
	4	15.8%|±7/2〉+ 10.9%|±5/2〉+ 25.1|±3/2〉+ 48.2%|±1/2〉

1. O. V. Dolomanov, L. J. Bourhis, R. J. Gildea, J. A. K. Howard and H. Puschmann, *J. Appl. Crystallogr.*, 2009, **42**, 339-341.
2. A. L. Spek, *Acta Cryst.*, 2009, **D65**, 148–155.
3. C. Chipot, R. Jaffe, B. Maigret, D. A. Pearlman and P. A. Kollman, *J. Am. Chem. Soc.*, 1996, **118**, 11217-11224.
4. T. Chen, M. Li and J. Liu, *Cryst. Growth Des.*, 2018, **18**, 2765-2783.